

Structure of the Nucleon*

M. Gökeler^{ab}, T.R. Hemmert^c, R. Horsley^d, D. Pleiter^e, P.E.L. Rakow^f, A. Schäfer^b, G. Schierholz^{eg}
 and W. Schroers^h

QCDSF Collaboration

^aInstitut für Theoretische Physik, Universität Leipzig, D-04109 Leipzig, Germany

^b Institut für Theoretische Physik, Universität Regensburg, D-93040 Regensburg, Germany

^cPhysik-Department, Theoretische Physik, Technische Universität München, 85747 Garching, Germany

^dSchool of Physics, University of Edinburgh, Edinburgh EH9 3JZ, UK

^eJohn von Neumann-Institut für Computing NIC, Deutsches Elektronen-Synchrotron DESY, 15738 Zeuthen, Germany

^fTheoretical Physics Division, Department of Mathematical Sciences, University of Liverpool, Liverpool L69 3BX, UK

^gDeutsches Elektronen-Synchrotron DESY, 22603 Hamburg, Germany

^hCenter for Theoretical Physics, Massachusetts Institute of Technology, Cambridge, MA 02139, USA

Generalized parton distributions provide information on the longitudinal and transverse distribution of partons in the fast moving nucleon. Furthermore, they contain information on the spin structure of the nucleon. First results of a lattice study of generalized parton distributions are presented.

1. INTRODUCTION

Understanding the internal structure of hadrons in terms of quarks and gluons (partons), and in particular how quarks and gluons provide the binding and spin of the nucleon, is one of the outstanding problems in particle physics.

Electromagnetic form factors provide information on the spatial distribution of charge and magnetization in the nucleon, irrespective of the partons' momenta and independent of the resolution scale. Parton distributions measure the probability $|\psi(x)|^2$ of finding a parton with frac-

tional longitudinal momentum x in the fast moving nucleon at a given transverse resolution $1/Q$, while no information on the transverse distribution of partons is provided. Generalized parton distributions (GPDs) [1] describe the coherence of two different hadron wave functions $\psi^\dagger(x + \xi/2) \psi(x - \xi/2)$, one where the parton carries fractional momentum $x + \xi/2$ and one where this fraction is $x - \xi/2$, from which further information on the transverse distribution of partons can be drawn [2]. In the limit where the momentum transfer Δ on the nucleon is purely transverse, i.e. $\Delta = (0, \Delta_\perp)$ and $\xi = \eta = 0$, GPDs regain a probabilistic interpretation [3]. When Fourier transformed to impact parameter

*Talk presented by G. Schierholz at LHP2003, Cairns, Australia.

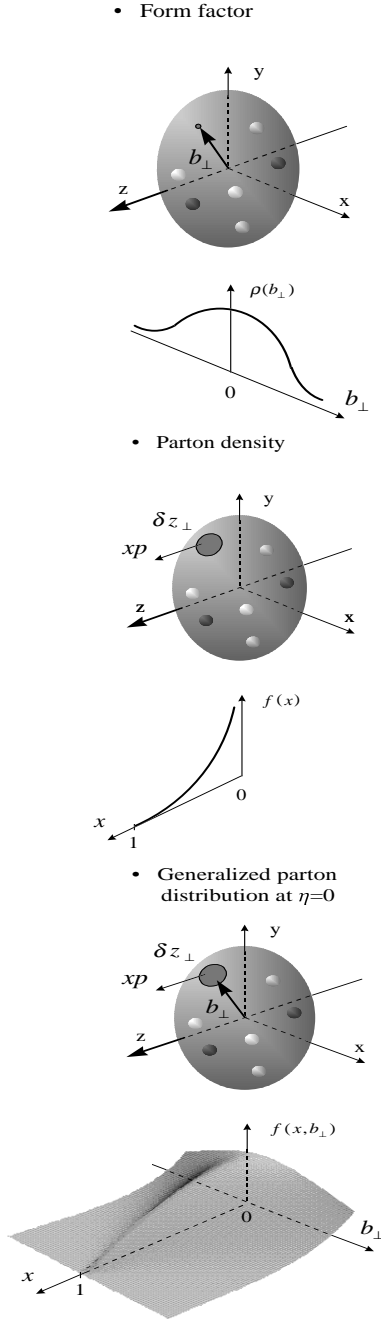


Figure 1. Probabilistic interpretation of form factors, parton distributions and generalized parton distributions at $\eta = 0$ [4] in the infinite momentum frame (resolution: $\delta z_{\perp} = 1/Q$).

space, they measure, for example, the probability of finding a parton of momentum fraction x at the impact parameter \mathbf{b}_{\perp} . In Fig. 1 we compare the information provided by form factors, parton distributions and GPDs. In other words, GPDs extend the well-known Feynman parton distribution and electromagnetic form factors of the nucleon to new kinematic dimensions. In the forward limit ($\Delta = 0$), these distributions reduce to the Feynman parton distributions.

Moments of GPDs are amenable to lattice calculations [5,6]. Thus, they offer promising ways to link phenomenological observations to first principle theoretical considerations. In this talk we will report on recent quenched results obtained by the QCDSF collaboration [5]. The calculation employs non-perturbatively improved Wilson fermions and non-perturbative renormalization factors [7] of the operators whose matrix elements are involved. Generally, improved Wilson fermions show only a very mild cut-off dependence [8]. We may therefore restrict ourselves to calculations done on the $16^3 \times 32$ lattice at $\beta = 6.0$.

2. (GENERALIZED) FORM FACTORS

We shall consider the GPDs H_q and E_q in the nucleon, where $q = u, d, \dots$ denotes the flavor of the struck quark. We will not consider the gluon sector here.

The zeroth moments of H_q and E_q give the electromagnetic Dirac and Pauli form factors:

$$\int_{-1}^1 dx H_q(x, \xi, \Delta^2) = F_1^q(\Delta^2),$$

$$\int_{-1}^1 dx E_q(x, \xi, \Delta^2) = F_2^q(\Delta^2).$$
(1)

Both form factors have been computed on the lattice [8,9]. In Fig. 2 we show a typical result for the Dirac form factor of the proton, $F_1 = F_1^u + F_1^d$. The solid curve is a dipole fit of the form

$$F_1(\Delta^2) = F_1(0)/(1 - \Delta^2/M_1^2)^2. \quad (2)$$

In Fig. 3 the dipole mass M_1 is extrapolated to the physical pion mass. We find good agreement

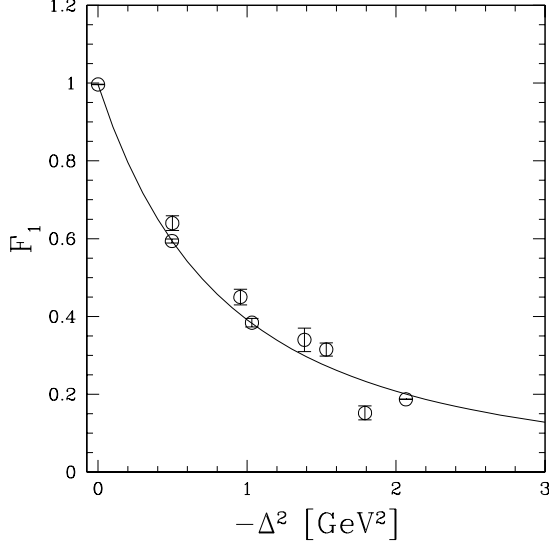


Figure 2. The Dirac form factor $F_1(\Delta^2)$ of the proton at $m_\pi = 450$ MeV, together with a dipole fit.

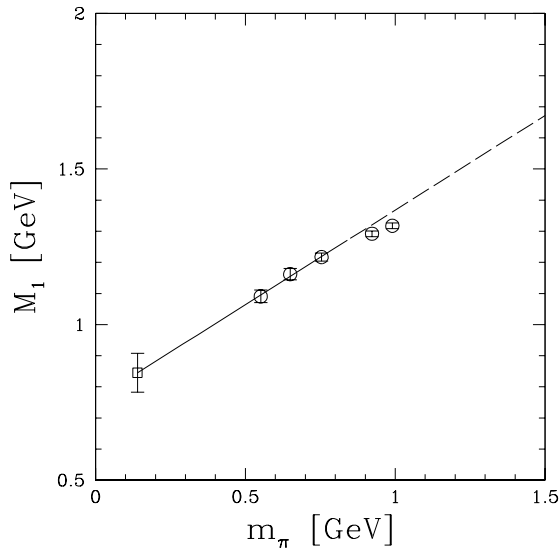


Figure 3. The dipole mass M_1 as a function of m_π , together with a linear extrapolation to the physical pion mass (\square).

with the phenomenological value, which is approximately equal to the physical ρ and ω mass.

The first moment gives us generalized form factors of a class of tensor operators:

$$\begin{aligned} \int_{-1}^1 dx x H_q(x, \xi, \Delta^2) &= A_2^q(\Delta^2) + \xi^2 C_2^q(\Delta^2), \\ \int_{-1}^1 dx x E_q(x, \xi, \Delta^2) &= B_2^q(\Delta^2) - \xi^2 C_2^q(\Delta^2), \end{aligned} \quad (3)$$

where $A_2^q(\Delta^2)$, $B_2^q(\Delta^2)$ and $C_2^q(\Delta^2)$ are given by the nucleon matrix elements of the energy-momentum tensor (EMT):

$$\begin{aligned} \langle p' | \mathcal{O}_{\{\mu\nu\}}^q | p \rangle &\equiv \frac{i}{2} \langle p' | \bar{q} \gamma_{\{\mu} \overleftrightarrow{D}_{\nu\}} q | p \rangle \\ &= A_2^q(\Delta^2) \bar{u}(p') \gamma_{\{\mu} \bar{p}_{\nu\}} u(p) \\ &\quad - B_2^q(\Delta^2) \frac{i}{2m_N} \bar{u}(p') \Delta^\alpha \sigma_{\alpha\{\mu} \bar{p}_{\nu\}} u(p) \\ &\quad + C_2^q(\Delta^2) \frac{1}{m_N} \bar{u}(p') u(p) \Delta_{\{\mu} \Delta_{\nu\}}. \end{aligned} \quad (4)$$

Here m_N denotes the nucleon mass, $\bar{p} = \frac{1}{2}(p' + p)$, $\Delta = p' - p$, and curly brackets refer to symmetrization of indices and subtraction of traces. The EMT has twist two and spin two. It is assumed to be renormalized at the scale Q , which makes $A_2^q(\Delta^2)$, $B_2^q(\Delta^2)$ and $C_2^q(\Delta^2)$ scale and scheme dependent. For the classification of states of definite J^{PC} contributing to (4) in the t -channel see [10]. The so-called skewedness parameter ξ is defined by $\xi = -n \cdot \Delta$, where n is a light-like vector with $n \cdot \bar{p} = 1$, and bounded by $|\xi| \leq 2\sqrt{\Delta^2}/(\Delta^2 - 4m_N^2)$. In the forward limit, $\Delta^2 = \xi = 0$, the first moment of H_q reduces to the first moment of the unpolarized parton distribution:

$$A_2^q(0) = \langle x_q \rangle \equiv \int_0^1 dx x (q_\uparrow(x) + q_\downarrow(x)), \quad (5)$$

where $q_{\uparrow(\downarrow)}(x)$ is the distribution with quark spin parallel (antiparallel) to the spin of the nucleon. Furthermore, we have [11]

$$\frac{1}{2}(A_2^q(0) + B_2^q(0)) = J_q, \quad (6)$$

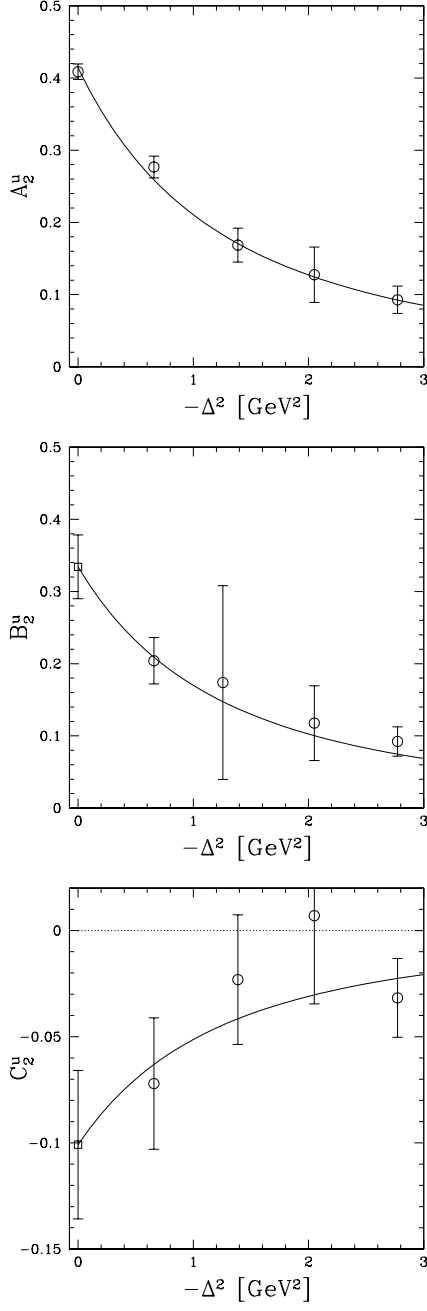


Figure 4. The generalized form factors A_2^u , B_2^u and C_2^u at $m_\pi = 450$ MeV, together with the dipole fit and the extrapolated values at $\Delta^2 = 0$ (\square).

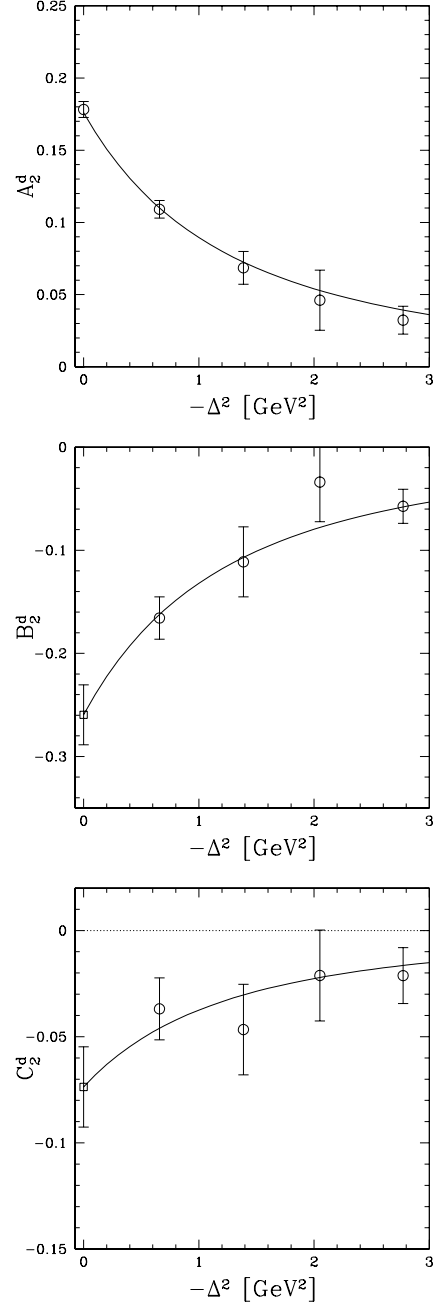


Figure 5. The generalized form factors A_2^d , B_2^d and C_2^d at $m_\pi = 450$ MeV, together with the dipole fit and the extrapolated values at $\Delta^2 = 0$ (\square).

where J_q is the angular momentum of the q quark, and

$$J = \sum_q J_q \quad (7)$$

is the total angular momentum of the nucleon carried by the quarks.

In Figs. 4 and 5 we show the generalized form factors $A_2^u(\Delta^2)$, $B_2^u(\Delta^2)$, $C_2^u(\Delta^2)$ and $A_2^d(\Delta^2)$, $B_2^d(\Delta^2)$, $C_2^d(\Delta^2)$ of the proton, again for $m_\pi = 450$ MeV. As for the nucleon form factors, the generalized form factors can be well described by the dipole ansatz

$$A_2^q(\Delta^2) = A_2^q(0)/(1 - \Delta^2/M^2)^2, \quad (8)$$

and similarly for B_2^q and C_2^q . The numbers refer to the \overline{MS} scheme at the renormalization scale $Q = 2$ GeV. Fits of $A_2^u(\Delta^2)$ and $A_2^d(\Delta^2)$ give the same dipole mass M within errors. We therefore fit our data by a common dipole mass M , only depending on the quark mass. For a reliable extrapolation to $\Delta^2 = 0$ it is important to cover a

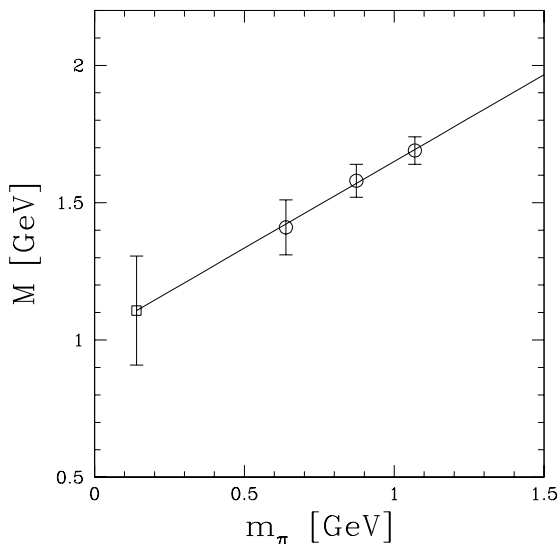


Figure 6. The dipole mass M as a function of m_π , together with a linear extrapolation to the physical pion mass (\square).

wide enough range of Δ^2 . Our data do not favor a monopole behavior.

In Fig. 6 we show the dipole mass M as a function of the pion mass. Again, the numbers appear to lie on a straight line. A linear extrapolation in m_π to the physical pion mass gives $M = 1.1(2)$ GeV. This value is close to the physical masses of the f_2 and a_2 mesons, which supports the hypothesis of tensor meson dominance. The numbers $A_2^q(0)$, $B_2^q(0)$ and $C_2^q(0)$ show little variation with the quark mass and are extrapolated quadratically in m_π to the physical pion mass. We obtain

q	$A_2^q(0)$	$B_2^q(0)$	$C_2^q(0)$
u	0.400(22)	0.334(113)	-0.134(81)
d	0.147(11)	-0.232(77)	-0.071(42)

Higher moments of H_q and E_q may be obtained in a similar way. Knowing sufficiently many moments, we can reconstruct $H_q(x, \xi, \Delta^2)$ and $E_q(x, \xi, \Delta^2)$ by inverse Mellin transform [12].

3. NUCLEON ANGULAR MOMENTUM

The angular momentum decomposes, in a gauge invariant way, into two contributions:

$$J_q = L_q + S_q, \quad (9)$$

where L_q is the orbital angular momentum and

$$S_q = \frac{1}{2}\Delta q \equiv \frac{1}{2} \int_0^1 dx (q_\uparrow(x) - q_\downarrow(x)) \quad (10)$$

is the spin of the quark. We know Δq from separate calculations [13,14], so that L_q can be computed from (6).

In Fig. 7 we show the total angular momentum $J = J_u + J_d$. The dependence on the pion mass is rather flat, as expected [15]. The errors are due to the relatively large statistical errors of B_2^u and B_2^d and the fact that B_2^u and B_2^d cancel to a large extent. A quadratic extrapolation in m_π to the physical pion mass gives

J	J_u	J_d	S_u	S_d
0.33(7)	0.37(6)	-0.04(4)	0.42(1)	-0.12(1)

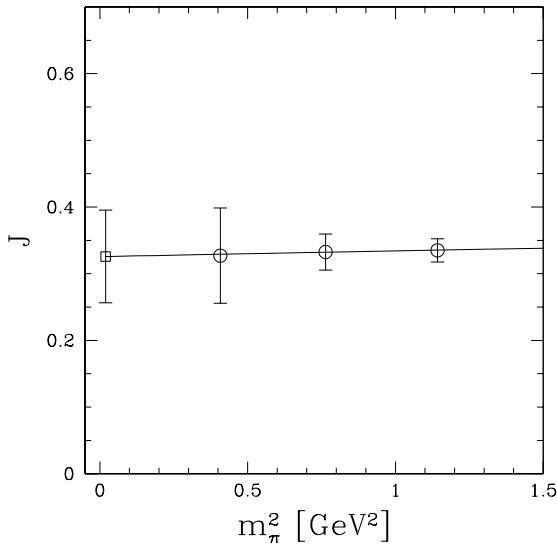


Figure 7. The total angular momentum J , together with a quadratic extrapolation to the physical pion mass (\square).

The numbers for S_q refer to our latest results [16], computed from the non-perturbatively improved axial vector current with non-perturbative renormalization factors. It turns out that the total angular momentum J carried by the quarks amounts to $\approx 70\%$ of the spin of the (quenched) proton, leaving a contribution of $\approx 30\%$ for the gluons. The major contribution is given by the u quark, while the contribution of the d quark is found to be negligible, which hints at strong pairing effects.

From J and S we can compute L_q now. The total orbital angular momentum of the (valence) quarks turns out to be consistent with zero:

$$L \equiv L_u + L_d = 0.03(7). \quad (11)$$

This indicates that (at virtuality $Q = 2 \text{ GeV}$) the parton's transverse momentum in the (quenched) proton is small.

4. GENERALIZED PARTON DISTRIBUTION

If the dipole behavior (2), (8) continues to hold for the higher moments as well, and if we assume that the dipole masses continue to grow in a Regge-like fashion, we may write

$$\int_{-1}^1 dx x^n H_q(x, 0, \Delta^2) = \langle x_q^n \rangle / (1 - \Delta^2 / M_{n+1}^2)^2, \quad (12)$$

with

$$M_l^2 = \text{const.} + l/\alpha', \quad (13)$$

where $\text{const.} \approx -0.5 \text{ GeV}^2$ and $1/\alpha' \approx 1.1 \text{ GeV}^2$. We know $\langle x_q^n \rangle$ from previous lattice calculations for $0 \leq n \leq 3$ [17]. That is sufficient to compute $H_q(x, 0, \Delta^2)$ by means of an inverse Mellin transform [12].

Having done so, the desired probability distribution of finding a parton of momentum fraction x at the impact parameter \mathbf{b}_\perp (see Fig. 1) is then obtained by the Fourier transform of $H_q(x, 0, \Delta^2)$:

$$H_q(x, 0, \mathbf{b}_\perp^2) = \frac{1}{(2\pi)^2} \int d^2 \Delta_\perp e^{i\mathbf{b}_\perp \cdot \Delta_\perp} H_q(x, 0, \Delta_\perp^2). \quad (14)$$

In Fig. 8 we show a first attempt at a lattice calculation of $H_q(x, 0, \mathbf{b}_\perp^2)$ for the u quark distribution in the proton. The volume under the two-dimensional surface (taken over the full kinematical range $0 \leq x \leq 1$ and $-\infty \leq b \leq \infty$) gives us back $\langle x_u \rangle$. We see that at smaller values of x the distribution in \mathbf{b}_\perp is rather broad (and different from the distribution sketched in Fig. 1), while at larger values of x it becomes somewhat more narrow. We also notice that the peak of the distribution is shifted slightly towards larger values of x as $|\mathbf{b}_\perp|$ is increased.

5. CONCLUSION

We have presented a first quenched lattice estimate of the generalized parton distribution

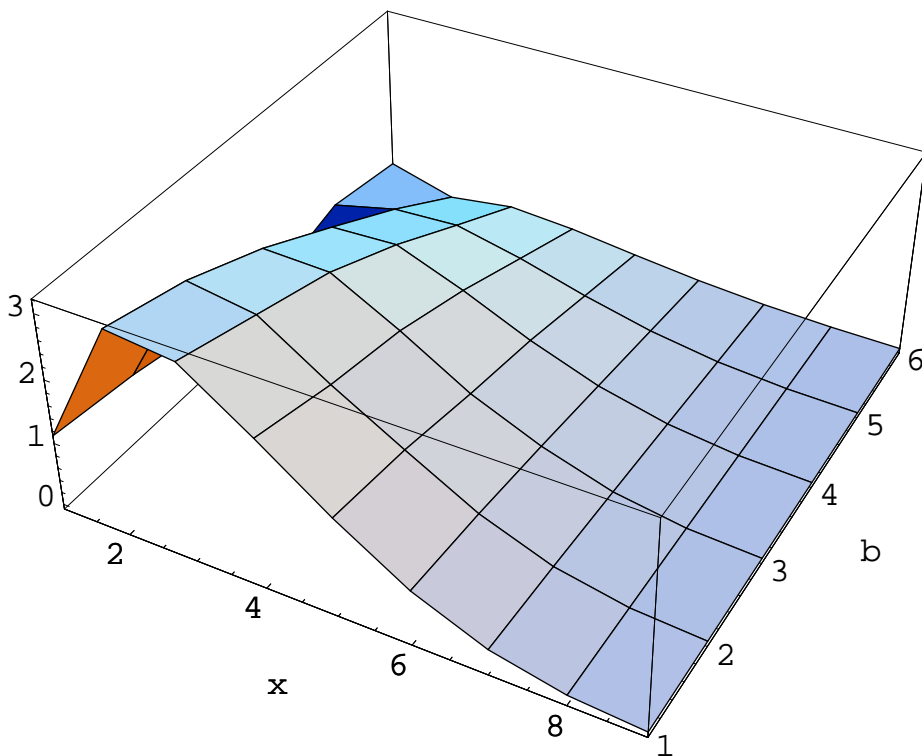


Figure 8. The generalized parton distribution $xH_u(x, 0, \mathbf{b}_\perp^2)$ as a function of x and the impact parameter $b = |\mathbf{b}_\perp|$. The plot extends over the range $0.1 \leq x \leq 0.9$ and $0.1 \text{ fm} \leq b \leq 0.6 \text{ fm}$.

$H_q(x, 0, \mathbf{b}_\perp^2)$, assuming that the generalized form factors of the higher operators (i.e. higher than the tensor operator) can be described by a dipole ansatz as well, with dipole masses lying on a Regge trajectory. As a by-product we obtained the total and orbital angular momentum of the nucleon carried by quarks. A calculation of the missing generalized form factors is in progress.

ACKNOWLEDGEMENTS

We like to thank the organizers of LHP2003, and in particular Alex Kalloniatis, for a most productive and pleasant workshop, and hope for many more to come. This work is supported in part by DFG and the EC under contract HPRN-

CT-2000-00145. WS is supported by a Feodor-Lynen fellowship and the U.S. Department of Energy under cooperative research agreement DF-FC02-94ER40818. The numerical calculations have been performed on the APE100 at NIC (Zeuthen) and T3E at NIC (Jülich). We thank Dieter Müller for providing Figure 1.

REFERENCES

1. D. Müller et al., Fortsch. Phys. 42, 101 (1994); X. Ji, Phys. Rev. Lett. 78, 610 (1997); A.V. Radyushkin, Phys. Rev. D56, 5524 (1997); M. Diehl et al., Phys. Lett. B411, 193 (1997); X. Ji, J. Phys. G24, 1181 (1998); J. Blümlein, B. Geyer and D. Robaschik, Nucl. Phys. B560, 283 (1999).

2. M. Diehl, Eur. Phys. J. C25, 223 (2002); M. Burkardt, Int. J. Mod. Phys. A18, 173 (2003).
3. M. Burkardt, Ref. [2].
4. A.V. Belitsky and D. Müller, Nucl. Phys. A711 (2002) 118c.
5. M. Göckeler et al., hep-ph/0304249.
6. P. Hägler et al., Phys. Rev. D68 (2003) 034505.
7. G. Martinelli et al., Nucl. Phys. B445 (1995) 81; M. Göckeler et al., Nucl. Phys. B544 (1999) 699.
8. M. Göckeler et al., hep-lat/0303019.
9. J.D. Ashley et al., hep-lat/0308024.
10. X. Ji and R.F. Lebed, Phys. Rev. D63, 076005 (2001).
11. X. Ji, Phys. Rev. Lett. 78, 610 (1997).
12. M. Göckeler et al., hep-ph/9711245.
13. M. Göckeler et al., Phys. Rev. D53, 2317 (1996); C. Best et al., hep-ph/9706502; M. Göckeler et al., Phys. Lett. B414 (1997) 340; S. Capitani et al., Nucl. Phys. (Proc. Suppl.) 79 (1999) 548; M. Göckeler et al., in preparation.
14. M. Fukugita et al., Phys. Rev. Lett. 75, 2092 (1995); S.J. Dong, J.-F. Lagaë and K.F. Liu, Phys. Rev. Lett. 75, 2096 (1995); S. Capitani et al., Nucl. Phys. (Proc. Suppl.) 79, 548 (1999); S. Güsken et al., Phys. Rev. D59, 114502 (1999); D. Dolgov et al., Phys. Rev. D66, 034506 (2002).
15. J.-W. Chen and X. Ji, Phys. Rev. Lett. 88, 052003 (2002).
16. M. Göckeler et al., in preparation.
17. M. Göckeler et al., Phys. Rev. D53, 2317 (1996); D. Dolgov et al., Phys. Rev. D66 (2002) 034506. M. Göckeler et al., Nucl. Phys. (Proc. Suppl.) 119 (2003) 32; M. Göckeler et al., in preparation.